HHS Public Access

Author manuscript

Cancer Res. Author manuscript; available in PMC 2020 June 15.

Published in final edited form as:

Cancer Res. 2019 December 15; 79(24): 6126–6138. doi:10.1158/0008-5472.CAN-19-0950.

Mcl-1 interacts with Akt to promote lung cancer progression

Guo Chen[1,&,#], **Dongkyoo Park**[1,&], **Andrew T. Magis**[2], **Madhusmita Behera**[3], **Suresh S. Ramalingam**[3], **Taofeek K. Owonikoko**[3], **Gabriel L. Sica**[4], **Keqiang Ye**[4], **Chao Zhang**[5], **Zhengjia Chen**[5], **Walter J. Curran**[1], **Xingming Deng**[1,*]

[1]Department of Radiation Oncology, Emory University School of Medicine and Winship Cancer Institute of Emory University, Atlanta, Georgia 30322, USA.

[2]Institute for Systems Biology, Seattle, WA 98109, USA

[3]Department of Hematology and Medical Oncology, Emory University School of Medicine and Winship Cancer Institute of Emory University, Atlanta, Georgia 30322, USA.

[4]Department of Pathology and Laboratory Medicine, Emory University School of Medicine and Winship Cancer Institute of Emory University, Atlanta, Georgia 30322, USA.

[5]Department of Biostatistics & Bioinformatics, Emory University School of Medicine and Winship Cancer Institute of Emory University, Atlanta, Georgia 30322, USA.

Abstract

Mcl-1 is a unique antiapoptotic Bcl-2 family protein that functions as a gatekeeper in manipulating apoptosis and survival in cancer cells. Akt is an oncogenic kinase that regulates multiple cellular functions and its activity is significantly elevated in human cancers. Here we discovered a cross-talk between Mcl-1 and Akt in promoting lung cancer cell growth. Depletion of endogenous Mcl-1 from human lung cancer cells using CRISPR/Cas9 or Mcl-1 shRNA significantly decreased Akt activity leading to suppression of lung cancer cell growth in vitro and in xenografts. Mechanistically, Mcl-1 directly interacted via its PEST domain with Akt at the pleckstrin homology (PH) domain. It is known that the interactions between the PH domain and kinase domain (KD) are important for maintaining Akt in an inactive state. The binding of Mcl-1/PH domain disrupted intramolecular PH/KD interactions to activate Akt. Intriguingly, Mcl-1 expression correlated with Akt activity in tumor tissues from non-small cell lung cancer patients. Using the Mcl-1-binding PH domain of Akt as a docking site, we identified a novel small molecule, PH-687, that directly targets the PH domain and disrupts Mcl-1/Akt binding, leading to suppression of Akt activity and growth inhibition of lung cancer in vitro and in vivo. By targeting the Mcl-1/Akt interaction, this mechanism-driven agent provides a highly attractive strategy for the treatment of lung cancer.

[*]**Corresponding Author**: Xingming Deng, Division of Cancer Biology, Department of Radiation Oncology, Emory University School of Medicine, Winship Cancer Institute of Emory University, Atlanta, GA 30322, USA. Phone: (404)778-3398, xdeng4@emory.edu, Fax: (404)778-1909.

[#]Present Address: Department of Medical Biochemistry and Molecular Biology, School of Medicine, Jinan University, 510632 Guangzhou, Guangdong, China.

[&]These authors contribute equally to this work and share first author

Disclosure of Potential Conflicts of Interest

The authors disclose no potential conflicts of interest

Introduction

Mcl-1 is a unique Bcl-2 family member that restricts the proapoptotic functions of BH123 multidomain *(i.e.* Bax and Bak) and BH3-only (*i.e.* Bim, Puma, tBid, etc.) proapoptotic molecules (1). Mcl-1 acts as a gatekeeper that is mainly located within the outer mitochondrial membrane (2). In addition to its canonical antiapoptotic function, Mcl-1 also has multiple other functions. Overexpression of Mcl-1 has been shown to inhibit autophagy, while downregulation of Mcl-1 is associated with the induction of autophagy (3–5). Mcl-1 is involved in controlling mitochondrial energy metabolism *(i.e.* ATP production) and respiration (6). Mcl-1 also regulates ATR-mediated CHK1 phosphorylation (7–9) and supports homologous recombination (HR)-mediated double-strand break (DSB) repair (10). Loss of Mcl-1 in mice resulted in peri-implantation embryonic lethality without cell apoptosis (11). Intriguingly, Mcl-1 plays a dual role in tumorigenesis. Mcl-1 transgenic mice have been reported to exhibit a high incidence of B-cell lymphoma (12). Hepatocyte-specific deletion of Mcl-1 triggers proliferation and hepatocarcinogenesis in mice (13).

Structurally, Mcl-1 has a long N-terminal end and lacks a typical BH4 domain compared with Bcl-2, Bcl-xL and Bcl-w (14). Mcl-1 encodes a long proline-, glutamic acid-, serine-, and threonine-rich (PEST) region upstream of the Bcl2 homology (BH) domain (15), which is associated with its short half-life (30 min-3h) and short-term pro-survival function (16). Mcl-1 is amplified and overexpressed in various cancers (17), including small cell lung cancer (SCLC), non-small cell lung cancer (NSCLC) (15, 18), leukemia (19), lymphoma (20), hepatocellular carcinoma (21), etc., which renders Mcl-1 a promising therapeutic target for various types of cancers (22–24).

Akt functions as an oncogenic kinase that consists of an N-terminal pleckstrin homology (PH) domain, a kinase domain (KD), and a C-terminal regulatory region carrying a hydrophobic motif (25–28). In response to growth factor stimulation, activation of PI3K produces phosphatidylinositol-3, 4, 5-bisphosphate (PIP3) that directly binds to the PH domain and induces a conformational change in Akt, which enables PDK1 or mTORC2 to access and phosphorylate Akt at T308 within the catalytic domain or at S473 in the hydrophobic motif, respectively (27, 29). Phosphorylation of T308 and S473 subsequently activates Akt and its downstream signaling (27, 30). Akt is normally maintained in an inactive state through intramolecular interaction between the PH and the KD. This domain-domain interaction prevents the Akt activation loop from being phosphorylated by PDK1 or mTORC2 (29). Here, we report the discovery that Mcl-1 directly interacts via its PEST domain with Akt at the PH domain, which disrupts intramolecular interactions between the PH domain and KD of Akt, leading to phosphorylation and activation of Akt and acceleration of lung cancer cell growth *in vitro* and *in vivo*. Based on discovery of this mechanism, we have identified a novel small molecule PH-687 that specifically targets the PH domain of Akt (*i.e.* the Mcl-1 binding region), disrupts Mcl-1/Akt interaction, inhibits Akt activity and exhibits strong antitumor activity against NSCLC *in vitro* and *in vivo*.

Materials and Methods

Materials

U6-Mcl-1gRNA-Cas9–2A-GFP plasmids, Duolink in situ PLA probe anti-rabbit plus (Duo92002), Duolink in situ PLA probe anti-Mouse minus (Duo92004) and Duolink in situ detection reagents FarRed (Duo92013) were purchased from Sigma (St. Louis, MO). BrdU cell proliferation kit and purified recombinant His tag-Akt protein (#14–276) were purchased from EMD Millipore (Billerica, MA). Purified recombinant His-tag-Mcl-1 protein (MCL1–781H) was obtained from Creative BioMart (Shirley, NY). Mcl-1 rabbit polyclonal Ab (sc-819), anti-β-actin (sc-47778), anti-Bax (sc-493), anti-HA (sc-7392) and anti-GFP (sc-9996) antibodies as well as Akt1/2 siRNA (sc-43609) were purchased from Santa Cruz Biotechnology (Dallas, Texas). Anti-pAkt S473 (#9271), anti-pAkt T308 (#13038), Akt (pan) mouse mAb (#2920), Mcl-1 (D2W9E) rabbit mAb (#94296), anti-pmTOR S2448 (#5536), anti-mTOR (#2983), anti-pP70S6K (#9234), anti-P70S6K (#2708), anti-Bcl-2 (#4223) and anti-Ki67 (#9027) antibodies were purchased from Cell Signaling Technology (Danvers, MA). EGF (PHG0311), IGF (PHG0071) and insulin (12585014) were obtained from ThermoFisher (Frederick, MD). WST-1 was purchased from Roche Diagnostics (Mannheim, Germany). Caspase-Glo® 3/7 assay kit was purchased from Promega Corporation (Madison, WI). Small molecule NSC128687 (PH-687) was obtained from the Drug Synthesis and Chemistry Branch, Developmental Therapeutic Program, Division of Cancer Treatment and Diagnosis, National Cancer Institute (NCI, Bethesda, MD) (http://dtp.nci.nih.gov/RequestCompounds). All reagents used were obtained from commercial sources unless otherwise stated.

Cell lines, plasmids and transfection

H1299, H460 and H157 cell lines were obtained from the American Type Culture Collection (ATCC, Manassas, VA) and were maintained in RPMI 1640 medium with 5% FBS and 5% bovine serum (BS). Two months after receipt, these cell lines were employed for the described experiments without further authentication by authors. Flag-tagged WT Mcl-1 in pCMV-Tag2A, and GFP-Akt PH domain/pcDNA3 (#18836) and 1036 pcDNA3 Myr HA Akt1 (#9008) were purchased from Addgene (Cambridge, MA). Gal4BD-AKT KD, VP16AD-AKT PH and pG5SEAP were kindly provided by Genentech, Inc. (South San Francisco, CA). Flag-tagged Mcl-1 deletion mutants, including ΔN (Δ10–120), ΔPEST (Δ120–200), ΔBH1 (Δ256–265), ΔBH2 (Δ305–315), ΔBH3 (Δ213–221) and ΔTM (Δ329–346), were generated by inverse PCR using WT Mcl-1 in pCMV-Tag2A as template as we recently described (10). GST-tagged WT Akt1, a series of Akt deletion mutants (i.e. GST-PH domain, GST-kinase domain, etc.) and HA-tagged WT Akt1 were kindly provided by Professor Keqiang Ye, Emory University School of Medicine. Various Mcl-1 or Akt DNA constructs were transfected into cells using NanoJuice (EMD Millipore, Billerica, MA) according to the manufacturer's instruction.

Knockout of Mcl-1 by CRISPR/Cas9

Mcl-1 was knocked out by CRISPR/Cas9 as we previously described (10). Briefly, H1299 cells were transfected with U6-Mcl-1gRNA-Cas9–2A-GFP plasmid (Sigma, St Louis, MO) using NanoJuice. The sequence of Mcl-1 targeting gRNA: 5'-GAT TAC CGC GTT TCT

TTT GAG G-3'. After transfection, GFP positive cells were sorted by flow cytometry and plated at a density of 1 cell per well in a 96-well plate. Mcl-1 expression of cells from a single clone was confirmed by Western blot.

Human phospho-kinase array

Human Phospho-Kinase Array Kit (Cat. # ARY003B) was purchased from R&D Systems (Minneapolis, MN). The human phospho-kinase array is a rapid, sensitive, and economical tool to simultaneously detect the relative levels of phosphorylation of 43 kinase phosphorylation sites and 2 related total proteins without performing numerous immunoprecipitations and Western blots. Capture and control antibodies have been spotted in duplicate on nitrocellulose membranes. Detailed procedures for the array were carried out according to the manufacturer's instruction. Briefly, cell lysates (500μg) isolated from H1299 parental or H1299 Mcl-$1^{-/-}$ cells were diluted and incubated overnight with the human phospho-kinase array. The array was washed to remove unbound proteins followed by incubation with a cocktail of biotinylated detection antibodies. Streptavidin-HRP and chemiluminescent detection reagents were applied and exposed to film. A signal is produced at each capture spot corresponding to the amount of phosphorylated protein bound. Phosphorylation levels of protein kinases were quantified by Image J.

Proximity Ligation Assay (PLA)

A Duolink® PLA system was purchased from Sigma-Aldrich (Saint Louis, MO). PLA was carried out for detection of Akt/Mcl-1 interaction in cells according to the manufacturer's instructions. Briefly, H1299 and H460 cells were plated in an 8-well chamber slide overnight, followed by fixation with methanol. After incubation with blocking solution, cells were incubated with Akt mouse monoclonal antibody (mAb) and Mcl-1 rabbit mAb at 4°C overnight. Cells were then incubated with Duolink in situ PLA probe anti-mouse minus and Duolink in situ PLA probe anti-rabbit plus for at 37°C for 60 min. Cells were incubated with the ligation solution at 37°C for 30 min, followed by incubation with the amplification solution for 100 min at 37°C. After washing, slides were mounted with a coverslip using Duolink® PLA mounting medium with DAPI. After 15min, PLA signals were detected by confocal fluorescence microscope (Leica Microsystems Inc.).

Mammalian two-hybrid assay

The mammalian two hybrid reporter plasmids for detection of the interaction between Akt kinase domain (KD) and PH domain, including Gal4BD-AKT KD, VP16AD-AKT PH and pG5SEAP, were kindly provided by Genentech Inc. The reporter assay for measurement of kinase domain/PH domain interaction was performed using secreted alkaline phosphatase (SEAP) Chemiluminescence Kit (Clontech, CA) according to the manufacturer's instruction and as previously described (27). Briefly, Gal4BD-AKT KD, VP16AD-AKT PH, pG5SEAP were co-transfected with empty vector (EV), flag-Mcl-1 WT, ΔPEST or PEST only into H1299 Mcl-$1^{-/-}$ cells. After 72h, culture medium from transfected cells was collected and mixed with SEAP substrate solution. Samples were then read on a chemiluminescence microplate reader (Spectramax Gemini, Molecular Devices, CA).

Treatment of lung cancer xenografts

All animal studies were undertaken in accordance with protocols approved by the Institutional Animal Care and Use Committee (IACUC) at Emory University (Atlanta, GA). Lung cancer xenografts were generated as previously described (31). Six-week-old male nude mice were purchased from Harlan (IN, US) and housed under pathogen-free conditions. 1×10^7 of H1299 cells were subcutaneously implanted into mouse flanks. Tumor bearing mice were randomly grouped and tumors were allowed to grow to an average volume of 100 mm^3 before treatment. Mice were treated with PH-687 through intraperitoneal injection (i.p) at the indicated dose. During treatment, tumor volumes were measured by caliper once every 4 days and calculated with the formula: $V = (L\times W^2)/2$ (L, length; W, width) as described (31).

Human patient samples and immunohistochemical (IHC) staining

Written informed consent was obtained from all human subjects, and use of human samples for IHC was approved by the Institutional Review Board of Emory University (IRB approval number 20081986). Paraffin-embedded human lung tissue samples from 208 NSCLC patients were obtained from the tissue bank at Emory University Winship Cancer Institute. Tissue microarray (TMA) was constructed with replicate cores of tumor and adjacent normal lung. After deparaffinization, rehydration, inactivation of endogenous peroxidase, and antigen retrieval, IHC staining was performed using R.T.U. Vectastain Kit (Vector Laboratories) according to the manufacturer's instructions. Primary antibody dilutions were: anti-Mcl-1 (1:300), anti-pAKT S473 (1:100), anti-pAKT T308 (1:100), anti-Ki67 (1:500) and anti-active caspase 3 (1:100). Ki67 positive cells and active caspase 3 positive cells in tumor tissues were scored at 400 × magnification. Percentage of positive cells was determined from three separate fields in each of three independent tumor samples. The semiquantitative evaluation of IHC staining of Mcl-1 and pAkt was carried out using an immunoscore based on both the percentage of stained cells and staining intensity as described (32). The intensity was defined as follows: 0, no appreciable staining; 1, weak intensity; 2, moderate intensity; 3, strong intensity; 4, very strong intensity. The immunoscore was calculated by multiplying the intensity by the percentage of positive staining, producing a total range of 0 to 400.

Statistical analysis

All data are presented as mean ± standard deviation (SD) from at least three independent experiments. Chi-square test and 2-tailed *t* test were performed to assess the statistical significance of differences between two groups. The correlation between Mcl-1 and pAkt expression was explored by using Pearson correlation analysis. For overall survival (OS), death from any cause was defined as the event. Time of OS was calculated as the time from study enrollment to death or last contact. For OS, patients were censored at time of last follow-up. OS rates of two patient groups stratified by each biomarker or other factors were estimated with the Kaplan-Meier method and compared between different groups using the log-rank test, respectively. The OS of each patient group at specific time points, such as 1 year, 3 years, and 5 years, etc. were also estimated alone with 95% CI. Cox proportional hazards models were further used in the multivariable analyses to assess adjusted effects of

biomarkers on the patients' OS after adjusting for other factors. The proportional hazards assumption was evaluated graphically and analytically with regression diagnostics. The significance level is set at 0.05 for all tests. All data management and statistical analysis were conducted using SAS Version 9.4 (SAS Institute, Inc., Cary, North Carolina).

Results

Mcl-1 loss leads to growth inhibition of cancer cells, which may occur through downregulation of Akt activity

To test the effects of Mcl-1 on cancer cell growth, endogenous Mcl-1 was knocked out from human lung cancer H1299 cells using CRISPR/Cas9 technology (Fig. 1A). Cell growth and colony formation were compared in H1299 parental vs. H1299 Mcl-1 $^{-/-}$ cells. Results indicate that depletion of endogenous Mcl-1 resulted in significant growth inhibition of H1299 cells (Fig. 1B and C). Protein kinase-mediated signaling pathways play critical roles in regulating cancer cell growth (26, 33–35). To assess whether Mcl-1 regulates protein kinase-mediated signaling pathways in human lung cancer cells, we employed a human phospho-kinase array to simultaneously detect the relative levels of phosphorylation of 43 kinase phosphorylation sites using total proteins isolated from H1299 parental vs. H1299 Mcl-1$^{-/-}$ cells. Intriguingly, among 43 kinases, significantly decreased levels of Akt phosphorylation at S473 and T308 were observed in H1299 Mcl-1$^{-/-}$ cells as compared to H1299 parental cells (Fig. 1D and E). No significant changes in phosphorylation levels of other kinases were observed in H1299 parental vs. H1299 Mcl-1$^{-/-}$ cells (Fig. 1D and E). These results suggest that Akt may act as a downstream signaling kinase in Mcl-1-mediated enhancement of cancer cell growth. It is well known that Akt activates mTOR/S6K signaling to promote cell growth (36). Thus, we were interested to test whether Mcl-1 loss affects the Akt downstream signaling pathway. As expected, knockout of Mcl-1 from H1299 cells or knockdown of Mcl-1 from another lung cancer cell line H460 cells resulted in decreased levels of pAkt, pmTOR and pS6K (Fig. 1F). These results suggest that Mcl-1 positively regulates Akt/mTOR signaling. It is well known that the canonical anti-apoptotic function of Mcl-1 occurs through interaction with proapoptotic proteins of Bcl-2 family proteins (37). Activation of Akt may be a new mechanism by which Mcl-1 regulates apoptosis and proliferation. In addition to cell growth, cell proliferation and caspase 3/7 activity were also measured in H1299 parental and H1299 Mcl-1$^{-/-}$ cells. Results indicate that knockout of Mcl-1 resulted in decreased cell proliferation and increased caspase3/7 activity (Supplementary Fig. S1).

To demonstrate whether Mcl-1 regulation of cancer cell growth occurs through Akt, a constitutively active form of Akt (Myr HA Akt1) (38) or empty vector was transfected into H1299 Mcl-1$^{-/-}$ cells, followed by colony formation assay. Knockout of Mcl-1 resulted in growth inhibition, and expression of the constitutively active form of Akt in H1299 Mcl-1$^{-/-}$ cells restored cell growth (Supplementary Fig. S2).

Mcl-1 loss retards tumor growth *in vivo*

To further evaluate the role of Mcl-1 in tumor growth *in vivo*, the same number (3×10^6) of H1299 parental or Mcl-1$^{-/-}$ H1299 cells were injected into subcutaneous tissue in the flank

region of nude mice to generate lung cancer xenografts (n=5 mice each group). Tumor volume was measured once every 3 days. Results indicate that depletion of Mcl-1 significantly inhibited growth of xenografted tumors (Fig. 2A and B), suggesting that Mcl-1 is a critical molecule for tumor growth. Intriguingly, IHC staining revealed that Mcl-1 deficiency was associated with decreased levels of pAkt and Ki67 (i.e. cell proliferation marker) and increased active caspase 3 (i.e. apoptosis marker) in tumor tissues (Fig. 2C–H). Decreased pAkt levels were also observed in H460 xenograft tumors expressing control shRNA or human Mcl-1 shRNA (Supplementary Fig. S3). These results indicate that Mcl-1/Akt signaling plays an important role in tumor growth.

The PEST domain of Mcl-1 interacts with the PH domain of Akt

To uncover the mechanism by which Mcl-1 regulates Akt, co-IP experiments using Mcl-1 or Akt antibody were performed in H1299 parental vs. H1299 Mcl-$1^{-/-}$ cells. Results indicate that Mcl-1 was associated with Akt protein in H1299 parental cells (Fig. 3A). Since Akt antibody could pull-down Mcl-1 protein only in H1299 parental but not in H1299 Mcl-$1^{-/-}$ cells (Fig. 3A), this indicates a potential direct interaction between Mcl-1 and Akt in human lung cancer cells. To further verify this interaction, similar co-IP experiments were carried out in a cell-free system using purified recombinant Mcl-1 and Akt proteins. Consistently, Mcl-1 also directly interacted with Akt in the cell-free system (Fig. 3B and C). To detect the intracellular localization(s) of Akt/Mcl-1 interaction, a Duolink® proximity ligation assay (PLA) system from Sigma-Aldrich was employed to detect Akt/Mcl-1 interaction in H1299 cells and H460 cells according to the manufacturer's instructions. Two primary antibodies raised in different species (i.e. Mcl-1 antibody from rabbit and Akt antibody from mouse) are used to detect two unique protein targets. A pair of oligonucleotide-labeled secondary antibodies (PLA probes) then binds to the primary antibodies. Hybridizing connector oligos join the PLA probes only if they are in close proximity to each other and ligase forms a closed circle DNA template that is required for rolling-circle amplification (RCA). The PLA probe then acts as a primer for a DNA polymerase, which generates concatemeric sequences during RCA. This allows up to 1000-fold amplified signal that is still tethered to the PLA probe, allowing localization of the signal. Labeled oligos hybridize to the complementary sequences within the amplicon. PLA signals were detected by fluorescence microscopy as discrete spots. Intriguingly, clear discrete spots were observed mainly in the cytoplasm, indicating that Mcl-1/Akt interactions in H1299 and H460 cells occur mainly in the cytoplasm (Fig. 3D). IgG, single Akt antibody alone and single Mcl-1 antibody alone were used as negative controls and no discrete spots were observed (Fig. 3D).

Mcl-1 contains multiple functional domains, including N-terminal, PEST, BH1, BH2, BH3 and transmembrane (TM) domains (14, 39). To identify the binding region of Mcl-1 to Akt, a panel of Flag-tagged Mcl-1 deletion mutants, including ΔN (10–120), ΔPEST (120–200), ΔBH1 (256–265), ΔBH2 (305–315), ΔBH3 (213–221) and ΔTM (329–346) (Fig. 3E), were employed for co-transfections with HA-Akt and co-IP experiments using Flag antibody. Results reveal that WT, ΔN, ΔBH1, ΔBH2, ΔBH3 and ΔTM but not ΔPEST Mcl-1 mutants, directly interacted with Akt protein (Fig. 3F), indicating that the PEST domain comprises the Akt binding site on Mcl-1 protein. Conversely, to further identify the Mcl-1 binding site on Akt protein, a series of GST-tagged Akt deletion mutants, including 1 (GST-PH domain),

2, 3, 4, 5, 6 (GST-kinase domain), 7, and 8 (WT) as shown in Fig. 3G, were used in co-transfections with Flag-tagged WT Mcl-1 and GST pull-down experiments. Intriguingly, WT (8) and Akt deletion mutants containing the PH domain (1, 3 and 7), but not Akt deletion mutants lacking the PH domain (2, 4, 5 and 6), could interact with WT Mcl-1 (Fig. 3H). These results demonstrate that the PH domain of the Akt protein is the Mcl-1 binding region.

Mcl-1/Akt binding is essential for Mcl-1 disruption of intramolecular PH/KD interactions, activation of Akt and promotion of tumor growth

It is well known that intramolecular pleckstrin homology (PH) domain/kinase domain (KD) interactions are important in maintaining AKT in an inactive state, and AKT activation is trigged by a conformational change that dislodges the PH from the KD (27).

Since Mcl-1 can directly interact with Akt at the PH domain (Fig. 3), we were interested to test whether Mcl-1 affects the intramolecular PH domain/KD interaction. GST-tagged KD, GFP-tagged PH domain and Flag-tagged WT Mcl-1 or ΔPEST Mcl-1 mutant were used for co-transfection and co-IP experiments. Results reveal that exogenous expression of WT Mcl-1 but not the PEST deletion mutant (ΔPEST) significantly reduced the interaction between PH domain and KD (Fig. 4A and B). To further confirm these findings, we employed a mammalian two-hybrid system to measure the PH/KD interaction. Co-transfection of Gal4BD-AKT KD and VP16AD-AKT PH along with pG5SEAP in cells drives the expression of secreted alkaline phosphatase (SEAP) when KD/PH interaction occurs. To test the effect of Mcl-1 on KD/PH interaction, the two-hybrid H1299 Mcl-$1^{-/-}$ cells were co-transfected with WT Mcl-1 or ΔPEST mutant Mcl-1, followed by analysis of SEAP activity. As expected, WT Mcl-1 but not ΔPEST mutant significantly reduced SEAP activity (Fig. 4C), which further confirmed the co-IP results. Since the PEST domain is required for Mcl-1/Akt binding, we propose that Mcl-1 disruption of intramolecular PH domain/kinase domain interactions may occur through Mcl-1/Akt binding.

PIP3 directly binds to the PH domain and induces a conformational change in Akt, which enables PDK1 or mTORC2 to access and phosphorylate Akt at T308 or S473 (33, 40). To test whether Mcl-1, similar to PIP3, may also affect the interactions between Akt and PDK1 or mTORC2, co-IP experiments using Akt antibody were performed in H1299 parental cells or H1299 Mcl-$1^{-/-}$ cells expressing WT Mcl-1, ΔPEST Mcl-1 mutant or empty vector, followed by Western blot using PDK1 or mTORC2 antibody, respectively. Results reveal that knockout of Mcl-1 disrupted Akt/PDK1 and Akt/mTORC2 interactions, and expression of WT Mcl-1 but not PEST deletion mutant restored Akt/PDK1 and Akt/mTORC2 interactions (Supplementary Fig. S4).

To test whether Mcl-1/Akt binding is essential for Mcl-1 regulation of Akt activity and cancer cell growth, WT Mcl-1 and PEST domain deletion mutant Mcl-1 (ΔPEST) were exogenously expressed in H1299 Mcl-$1^{-/-}$ cells, followed by analysis of pAkt, pmTOR, p-p70 S6K and colony formation. Expression of exogenous WT Mcl-1 but not the ΔPEST mutant Mcl-1 led to increased levels of pAkt, pmTOR and p-p70 S6K and promotion of cancer growth (Fig. 4D and E). To further assess whether deletion of PEST domain (*i.e.* Akt binding site) affects tumor growth, Mcl-1-deficient H1299 cells expressing exogenous WT

or ΔPEST mutant were employed to establish lung cancer xenografts. Expression of WT Mcl-1 significantly promoted tumor growth in xenograft models. Deletion of PEST from Mcl-1 ablated Mcl-1's capacity to promote tumor growth (Fig. 4F). These results indicate that Mcl-1/Akt binding is required for Mcl-1 to activate Akt and promote cancer growth.

Mcl-1 expression levels are correlated with pAkt levels in tumor tissues from NSCLC patients

The majority of our experiments employed human lung cancer cell lines (i.e. H1299 or H460) derived from non-small cell lung cancer (NSCLC), therefore, it was of interest to test whether Mcl-1 and pAkt are upregulated in tumor tissues from patients with NSCLC, and whether Mcl-1 expression is correlated with pAkt in NSCLC patient tumors. We analyzed Mcl-1 and pAkt in samples from 208 NSCLC patients by IHC staining employing anti-Mcl-1 or phospho-specific Akt (S473) antibody, respectively. NSCLC human tissue samples were obtained from the tissue bank at Emory University Winship Cancer Institute. Tissue microarrays (TMA) were generated with replicate cores of tumor and adjacent normal lung. Semiquantitative evaluation of IHC staining of Mcl-1 or pAkt was carried out using immunoscores based on both percentage of stained cells and staining intensity as previously described (32, 41, 42). Mcl-1 protein expression was significantly higher in tumor tissues compared to adjacent normal lung tissues (Fig. 5A). The observed levels of Mcl-1 were positively correlated with levels of pAkt in tumor tissues (r=0.662) (Fig. 5B and C). Importantly, elevated levels of Mcl-1 or pAkt in tumor tissues were significantly associated with poor overall survival for NSCLC patients (Fig. 5D and E), suggesting that Mcl-1 and pAkt, could be potential prognostic biomarkers of survival for NSCLC patients.

Small molecule PH-687 targets the PH Domain, disrupts Mcl-1/Akt interaction and inhibits Akt activity leading to growth inhibition of human lung cancer cells

We have demonstrated that interaction of Mcl-1 via its PEST domain with the PH domain of Akt leads to Akt activation by disrupting intramolecular interactions between its PH domain and KD (Figs 3 and 4), indicating that the PH domain (aa6–108) is an attractive target for screening of small molecules that may potentially disrupt Mcl-1/Akt binding. An NCI database library of 300,000 small molecules was docked into the PH structure pocket (aa6–108) identified by the UCSF DOCK 6.1 program suite for screening as we previously described (31). The small molecules were ranked according to their energy scores. The top 500 small molecules based on predicted binding energies were selected for screening of cytotoxicity in human lung cancer cells by sulforhodamine B (SRB) assay as previously described (43). Among these small molecules, the compound NSC 128687 ($C_9H_{12}N_3O_7P$, MW 305.18) had the most potent activity against human lung cancer cells. We named this lead compound PH-687. Molecular modeling of PH-687 in complex with the PH binding pocket in Akt is shown in Fig. 6A. To test whether PH-687 specifically binds to the PH domain in Akt, we generated recombinant GST-tagged WT Akt, PH deletion Akt mutant (ΔPH) and PH domain-only proteins (Fig. 6B) and measured PH-687 compound/Akt protein binding using thermal shift assay. Thermal shift assay is a technique to study protein/small molecule interactions that enhance protein thermal stability and increase melting temperatures (Tm) (44). Dose dependent increases in melting temperature (Tm) were observed when purified GST-WT Akt and GST-PH mutant proteins were incubated with

increasing concentrations of PH-678 (Fig. 6C). There was no significant increase in Tm when GST-ΔPH protein was incubated with increasing concentrations of PH-687 (Fig. 6C). These results indicate that small molecule PH-687 binds to the PH domain of Akt protein, and the PH domain is essential for this binding. Since PH-687 can bind to the Mcl-1 binding site (i.e. PH domain) on Akt protein, we tested the effect of PH-687 on Mcl-1/Akt interaction. Co-IP experiments reveal that treatment of H1299 cells with increasing concentrations of PH-687 resulted in a dose-dependent dissociation of Mcl-1/Akt complexes (Fig. 6D), indicating that PH-687 is able to disrupt Mcl-1/Akt interaction in H1299 cells. Importantly, PH-678-induced disruption of Mcl-1/Akt interaction significantly reduced Akt activity leading to growth inhibition in various human lung cancer cell lines (Fig. 6E–G).

To test whether PH-687-mediated Mcl-1/Akt dissociation enhances interaction between the PH and KD domains, we employed a mammalian two-hybrid system to measure the PH/KD interaction in H1299 cells using Gal4BD-AKT KD, VP16AD-AKT PH and pG5SEAP in the absence or presence of PH-687 as described above. Results reveal that treatment of H1299 cells with increasing concentrations (0, 0.5, 1, 2 μM) of PH-687 for 24h led to increased PH/KD interaction in a dose-dependent manner (Supplementary Fig. S5A). Intriguingly, treatment of H1299 cells with PH-687 also resulted in a dose-dependent decreased interaction of Akt with PDK1 or mTORC2 (Supplementary Fig. S5B).

To further test whether PH-687 specifically functions through targeting Mcl-1/AKT signaling in lung cancer cells, H1299 parental cells, H1299 Mcl-$1^{-/-}$ cells and H1299 cells expressing Akt siRNA were treated with increasing concentrations of PH-687 (0, 0.1, 0.5, 1μM), followed by colony formation assay. Results reveal that treatment of H1299 cells with increasing concentrations of PH-687 led to growth inhibition in a dose-dependent manner. In contrast, knockout of Mcl-1 by CRISPR/cas9 or knockdown of Akt by Akt siRNA reduced the inhibitory effect of PH-687 on cell growth (Supplementary Fig. S6), indicating that the effect of PH-687 occurs through Mcl-1/Akt signaling.

To test whether Mcl-1 or PH-687 also affects Akt activation by growth factors such as EGF, IGF or insulin, first, H1299 parental and H1299 Mcl-$1^{-/-}$ cells were treated with EGF (100ng/ml), IGF (10ng/ml) or insulin (1μg/ml) for 1h, followed by analysis of Akt phosphorylation. Results indicate that treatment of H1299 cells with EGF, IGF and insulin enhanced levels of pAkt S473 and pAkt T308. Knockout of Mcl-1 blocked EGF, IGF and insulin-induced Akt phosphorylation at S473 and T308. (Supplementary Fig. 7A). Second, H1299 cells were treated with EGF (100ng/ml), IGF (10ng/ml) or insulin (1μg/ml) in the absence or presence of PH-687 (2μM) for 1h, followed by analysis of Akt phosphorylation. Results reveal that PH-687 inhibited EGF, IGF and insulin-induced Akt phosphorylation at S473 and T308 (Supplementary Fig. S7B).

PH-687 has potent anti-tumor activity against NSCLC *in vivo*

To test the anti-tumor potency of PH-687 *in vivo*, nude mice with NSCLC (i.e. H1299) xenografts were treated with increasing doses (0, 30, 60 and 90 mg/kg/d) of PH-687 for 4 weeks. Treatment with PH-687 suppressed tumor growth in a dose-dependent manner *in vivo* (Fig. 7A). IHC staining of representative samples from harvested tumor tissues revealed that treatment of mice with PH-687 resulted in decreased levels of pAkt (S473), pAkt

(T308) and Ki67 in association with increased apoptosis (i.e. active caspase 3) (Fig. 7B and C). There was no significant weight loss and no significant increase in ALT, AST and BUN or reduction in WBC, RBC, hemoglobin and PLT in mice treated with PH-687 in the dose range of 30–90mg/kg/d. Histopathologic evaluation of harvested normal tissues (brain, heart, lung, liver, spleen, kidney and intestine) revealed no evidence of normal tissue toxicity (Supplementary Fig. S8).

Discussion

The PI3K/Akt pathway regulates multiple cellular functions, including cell growth, differentiation, proliferation, survival, motility, invasion and intracellular trafficking (45). AKT is frequently activated in cancers, which occurs through mutations of upstream genes like PIK3CA (46), PTEN (47) and KRAS (48, 49). Akt can also be activated through mutations within its PH domain (27). Here we discovered that Mcl-1 activates Akt in a mechanism independent of genomic alterations. Depletion of endogenous Mcl-1 from human lung cancer cells using CRISPR/Cas9 or Mcl-1 shRNA resulted in significant downregulation of Akt activity and suppression of lung cancer cell growth *in vitro* and *in vivo*. In contrast, overexpression of exogenous Mcl-1 enhanced Akt activity and promoted lung cancer cell growth. Intriguingly, our analysis of 208 NSCLC patient tumors revealed that higher levels of Mcl-1 are correlated with higher levels of pAkt in tumor tissues, which are associated with poor outcome of NSCLC patients. These findings strongly suggest that Mcl-1, in addition to its canonical antiapoptotic function via interaction with proapoptotic Bcl2 family proteins, may also directly regulate Akt to support cancer cell growth, which may negatively affect the prognosis of NSCLC patients.

Mechanistically, Mcl-1 directly interacts with Akt in lung cancer cells and in a cell-free system. Interaction between the PH and KD is important for maintaining the kinase in an inactive state (50). Mutations observed in human tumors in AKT at the PH–KD contact sites (*i.e.* L52R, Q79K, and D323H) can disrupt PH-KD interaction leading to activation of AKT in human cancers (27). Our domain-mapping studies reveal that Mcl-1 interacts directly via its PEST domain with Akt at the PH domain, and the binding of Mcl-1 with the PH domain can disrupt PH-KD interaction, leading to Akt activation. Importantly, Mcl-1/PH interaction not only activates Akt but also promotes lung cancer cell growth *in vitro* and *in vivo*. These findings uncover a novel mechanism of Akt activation that occurs through a PH mutation(s)-independent manner.

Because the PEST domain of Mcl-1 interacts directly with the PH domain of Akt, we can choose either the Mcl-1 PEST domain or the Akt PH domain as a docking site for the discovery of small molecules that could potentially disrupt Mcl-1/Akt interaction. We chose the PH domain as docking site for small molecule screening using the UCSF DOCK 6.1 program, and identified PH-687 as a lead compound that not only binds to the PH domain of Akt but also disrupts Mcl-1/Akt interaction, leading to inhibition of Akt activity. Importantly, PH-687 has potent antitumor activity against NSCLC *in vitro* and *in vivo*.

In summary, our findings have demonstrated that Mcl-1 interacts directly via its PEST domain with Akt at the PH domain leading to disruption of intramolecular PH-KD

interactions, which results in Akt activation in cancer cells. Thus, Mcl-1, in addition to its anti-apoptotic function, appears to function upstream of Akt and activates Akt signaling via direct interaction. Specifically targeting Mcl-1/Akt interaction by employing small molecules such as PH-687 represents a potentially new and effective strategy for cancer treatment.

Supplementary Material

Refer to Web version on PubMed Central for supplementary material.

Acknowledgments

This work was supported by NCI, National Institutes of Health grants R01CA193828, R01CA136534, R01CA200905 and P50CA217691(to X. Deng), by the Winship Research Informatics, Pathology and Integrated Cellular Imaging shared resource, the cores supported by the Winship Cancer Institute of Emory University (P30CAJ38292), by the Winship Fashion a Cure Research Scholar Award (to X. Deng), a philanthropic award provided by the Winship Cancer Institute of Emory University, and by Winship Endowment Fund (to X. Deng).

We thank Genentech, Inc. for kindly providing Gal4BD-AKT KD, VP16AD-AKT PH and pG5SEAP. We also thank Anthea Hammond for editing of the manuscript.

References

1. Czabotar PE, Lessene G, Strasser A, Adams JM. Control of apoptosis by the BCL-2 protein family: implications for physiology and therapy. Nature reviews Molecular cell biology. 2014;15:49–63. [PubMed: 24355989]
2. Kiraz Y, Adan A, Kartal Yandim M, Baran Y. Major apoptotic mechanisms and genes involved in apoptosis. Tumour biology : the journal of the International Society for Oncodevelopmental Biology and Medicine. 2016;37:8471–86. [PubMed: 27059734]
3. Elgendy M, Abdel-Aziz AK, Renne SL, Bornaghi V, Procopio G, Colecchia M, et al. Dual modulation of MCL-1 and mTOR determines the response to sunitinib. The Journal of clinical investigation. 2017;127:153–68. [PubMed: 27893461]
4. Elgendy M, Ciro M, Abdel-Aziz AK, Belmonte G, Dal Zuffo R, Mercurio C, et al. Beclin 1 restrains tumorigenesis through Mcl-1 destabilization in an autophagy-independent reciprocal manner. Nature communications. 2014;5:5637.
5. Germain M, Nguyen AP, Le Grand JN, Arbour N, Vanderluit JL, Park DS, et al. MCL-1 is a stress sensor that regulates autophagy in a developmentally regulated manner. The EMBO journal. 2011;30:395–407. [PubMed: 21139567]
6. Perciavalle RM, Stewart DP, Koss B, Lynch J, Milasta S, Bathina M, et al. Anti-apoptotic MCL-1 localizes to the mitochondrial matrix and couples mitochondrial fusion to respiration. Nature cell biology. 2012;14:575–83. [PubMed: 22544066]
7. Jamil S, Stoica C, Hackett TL, Duronio V. MCL-1 localizes to sites of DNA damage and regulates DNA damage response. Cell Cycle. 2010;9:2843–55. [PubMed: 20647761]
8. Pawlikowska P, Leray I, de Laval B, Guihard S, Kumar R, Rosselli F, et al. ATM-dependent expression of IEX-1 controls nuclear accumulation of Mcl-1 and the DNA damage response. Cell death and differentiation. 2010;17:1739–50. [PubMed: 20467439]
9. Jamil S, Mojtabavi S, Hojabrpour P, Cheah S, Duronio V. An essential role for MCL-1 in ATR-mediated CHK1 phosphorylation. Mol Biol Cell. 2008;19:3212–20. [PubMed: 18495871]
10. Chen G, Magis AT, Xu K, Park D, Yu DS, Owonikoko TK, et al. Targeting Mcl-1 enhances DNA replication stress sensitivity to cancer therapy. J Clin Invest. 2018;128:500–16. [PubMed: 29227281]
11. Rinkenberger JL, Horning S, Klocke B, Roth K, Korsmeyer SJ. Mcl-1 deficiency results in peri-implantation embryonic lethality. Genes & development. 2000;14:23–7. [PubMed: 10640272]

12. Zhou P, Levy NB, Xie H, Qian L, Lee CY, Gascoyne RD, et al. MCL1 transgenic mice exhibit a high incidence of B-cell lymphoma manifested as a spectrum of histologic subtypes. Blood. 2001;97:3902–9. [PubMed: 11389033]
13. Weber A, Boger R, Vick B, Urbanik T, Haybaeck J, Zoller S, et al. Hepatocyte-specific deletion of the antiapoptotic protein myeloid cell leukemia-1 triggers proliferation and hepatocarcinogenesis in mice. Hepatology. 2010;51:1226–36. [PubMed: 20099303]
14. Day CL, Chen L, Richardson SJ, Harrison PJ, Huang DC, Hinds MG. Solution structure of prosurvival Mcl-1 and characterization of its binding by proapoptotic BH3-only ligands. J Biol Chem. 2005;280:4738–44. [PubMed: 15550399]
15. Zhao J, Xin M, Wang T, Zhang Y, Deng X. Nicotine enhances the antiapoptotic function of Mcl-1 through phosphorylation. Mol Cancer Res. 2009;7:1954–61. [PubMed: 19903766]
16. Wang B, Xie M, Li R, Owonikoko TK, Ramalingam SS, Khuri FR, et al. Role of Ku70 in deubiquitination of Mcl-1 and suppression of apoptosis. Cell death and differentiation. 2014;21:1160–9. [PubMed: 24769731]
17. Xiang W, Yang CY, Bai L. MCL-1 inhibition in cancer treatment. OncoTargets and therapy. 2018;11:7301–14. [PubMed: 30425521]
18. Song L, Coppola D, Livingston S, Cress D, Haura EB. Mcl-1 regulates survival and sensitivity to diverse apoptotic stimuli in human non-small cell lung cancer cells. Cancer biology & therapy. 2005;4:267–76. [PubMed: 15753661]
19. Akgul C Mcl-1 is a potential therapeutic target in multiple types of cancer. Cell Mol Life Sci. 2009;66:1326–36. [PubMed: 19099185]
20. Schwickart M, Huang X, Lill JR, Liu J, Ferrando R, French DM, et al. Deubiquitinase USP9X stabilizes MCL1 and promotes tumour cell survival. Nature. 2010;463:103–7. [PubMed: 20023629]
21. Liao M, Zhao J, Wang T, Duan J, Zhang Y, Deng X. Role of bile salt in regulating Mcl-1 phosphorylation and chemoresistance in hepatocellular carcinoma cells. Mol Cancer. 2011;10:44. [PubMed: 21507240]
22. Song KA, Hosono Y, Turner C, Jacob S, Lochmann TL, Murakami Y, et al. Increased Synthesis of MCL-1 Protein Underlies Initial Survival of EGFR-Mutant Lung Cancer to EGFR Inhibitors and Provides a Novel Drug Target. Clinical cancer research : an official journal of the American Association for Cancer Research. 2018;24:5658–72. [PubMed: 30087143]
23. Campbell KJ, Dhayade S, Ferrari N, Sims AH, Johnson E, Mason SM, et al. MCL-1 is a prognostic indicator and drug target in breast cancer. Cell death & disease. 2018;9:19. [PubMed: 29339815]
24. Leverson JD, Zhang H, Chen J, Tahir SK, Phillips DC, Xue J, et al. Potent and selective small-molecule MCL-1 inhibitors demonstrate on-target cancer cell killing activity as single agents and in combination with ABT-263 (navitoclax). Cell death & disease. 2015;6:e1590. [PubMed: 25590800]
25. Vanhaesebroeck B, Alessi DR. The PI3K-PDK1 connection: more than just a road to PKB. Biochem J. 2000;346 Pt 3:561–76.
26. Hers I, Vincent EE, Tavare JM. Akt signalling in health and disease. Cell Signal. 2011;23:1515–27. [PubMed: 21620960]
27. Parikh C, Janakiraman V, Wu WI, Foo CK, Kljavin NM, Chaudhuri S, et al. Disruption of PH-kinase domain interactions leads to oncogenic activation of AKT in human cancers. Proc Natl Acad Sci U S A. 2012;109:19368–73. [PubMed: 23134728]
28. Hanada M, Feng J, Hemmings BA. Structure, regulation and function of PKB/AKT--a major therapeutic target. Biochim Biophys Acta. 2004;1697:3–16. [PubMed: 15023346]
29. Calleja V, Alcor D, Laguerre M, Park J, Vojnovic B, Hemmings BA, et al. Intramolecular and intermolecular interactions of protein kinase B define its activation in vivo. PLoS Biol. 2007;5:e95. [PubMed: 17407381]
30. Scheid MP, Woodgett JR. Unravelling the activation mechanisms of protein kinase B/Akt. FEBS Lett. 2003;546:108–12. [PubMed: 12829245]
31. Han B, Park D, Li R, Xie M, Owonikoko TK, Zhang G, et al. Small-Molecule Bcl2 BH4 Antagonist for Lung Cancer Therapy. Cancer cell. 2015;27:852–63. [PubMed: 26004684]

32. Liu Y, Sun SY, Owonikoko TK, Sica GL, Curran WJ, Khuri FR, et al. Rapamycin induces Bad phosphorylation in association with its resistance to human lung cancer cells. Mol Cancer Ther. 2012;11:45–56. [PubMed: 22057915]
33. Manning BD, Toker A. AKT/PKB Signaling: Navigating the Network. Cell. 2017;169:381–405. [PubMed: 28431241]
34. Kim D, Dan HC, Park S, Yang L, Liu Q, Kaneko S, et al. AKT/PKB signaling mechanisms in cancer and chemoresistance. Frontiers in bioscience : a journal and virtual library. 2005;10:975–87. [PubMed: 15569636]
35. Garcia-Gomez R, Bustelo XR, Crespo P. Protein-Protein Interactions: Emerging Oncotargets in the RAS-ERK Pathway. Trends in cancer. 2018;4:616–33. [PubMed: 30149880]
36. Dibble CC, Cantley LC. Regulation of mTORC1 by PI3K signaling. Trends in cell biology. 2015;25:545–55. [PubMed: 26159692]
37. Senichkin VV, Streletskaia AY, Zhivotovsky B, Kopeina GS. Molecular Comprehension of Mcl-1: From Gene Structure to Cancer Therapy. Trends Cell Biol. 2019;29:549–62. [PubMed: 31030977]
38. Sun M, Wang G, Paciga JE, Feldman RI, Yuan ZQ, Ma XL, et al. AKT1/PKBalpha kinase is frequently elevated in human cancers and its constitutive activation is required for oncogenic transformation in NIH3T3 cells. Am J Pathol. 2001;159:431–7. [PubMed: 11485901]
39. Bae J, Leo CP, Hsu SY, Hsueh AJ. MCL-1S, a splicing variant of the antiapoptotic BCL-2 family member MCL-1, encodes a proapoptotic protein possessing only the BH3 domain. J Biol Chem. 2000;275:25255–61. [PubMed: 10837489]
40. Yudushkin I Getting the Akt Together: Guiding Intracellular Akt Activity by PI3K. Biomolecules. 2019;9.
41. Jonat W, Maass H, Stegner HE. Immunohistochemical measurement of estrogen receptors in breast cancer tissue samples. Cancer Res. 1986;46:4296s–8s. [PubMed: 2425947]
42. Morote J, Fernandez S, Alana L, Iglesias C, Planas J, Reventos J, et al. PTOV1 expression predicts prostate cancer in men with isolated high-grade prostatic intraepithelial neoplasia in needle biopsy. Clin Cancer Res. 2008;14:2617–22. [PubMed: 18451224]
43. Park D, Magis AT, Li R, Owonikoko TK, Sica GL, Sun SY, et al. Novel small-molecule inhibitors of Bcl-XL to treat lung cancer. Cancer Res. 2013;73:5485–96. [PubMed: 23824742]
44. Jin L, Li D, Alesi GN, Fan J, Kang HB, Lu Z, et al. Glutamate dehydrogenase 1 signals through antioxidant glutathione peroxidase 1 to regulate redox homeostasis and tumor growth. Cancer Cell. 2015;27:257–70. [PubMed: 25670081]
45. Perez-Ramirez C, Canadas-Garre M, Molina MA, Faus-Dader MJ, Calleja-Hernandez MA. PTEN and PI3K/AKT in non-small-cell lung cancer. Pharmacogenomics. 2015;16:1843–62. [PubMed: 26555006]
46. Nicholson KM, Anderson NG. The protein kinase B/Akt signalling pathway in human malignancy. Cell Signal. 2002;14:381–95. [PubMed: 11882383]
47. Sansal I, Sellers WR. The biology and clinical relevance of the PTEN tumor suppressor pathway. J Clin Oncol. 2004;22:2954–63. [PubMed: 15254063]
48. Affolter A, Drigotas M, Fruth K, Schmidtmann I, Brochhausen C, Mann WJ, et al. Increased radioresistance via G12S K-Ras by compensatory upregulation of MAPK and PI3K pathways in epithelial cancer. Head Neck. 2013;35:220–8. [PubMed: 22302684]
49. Okudela K, Hayashi H, Ito T, Yazawa T, Suzuki T, Nakane Y, et al. K-ras gene mutation enhances motility of immortalized airway cells and lung adenocarcinoma cells via Akt activation: possible contribution to non-invasive expansion of lung adenocarcinoma. Am J Pathol. 2004;164:91–100. [PubMed: 14695323]
50. Calleja V, Laguerre M, Parker PJ, Larijani B. Role of a novel PH-kinase domain interface in PKB/Akt regulation: structural mechanism for allosteric inhibition. PLoS Biol. 2009;7:e17. [PubMed: 19166270]

Significance

Findings indicate that targeting Mcl-1/Akt interaction by employing small molecules such as PH-687 represents a potentially new and effective strategy for cancer treatment.

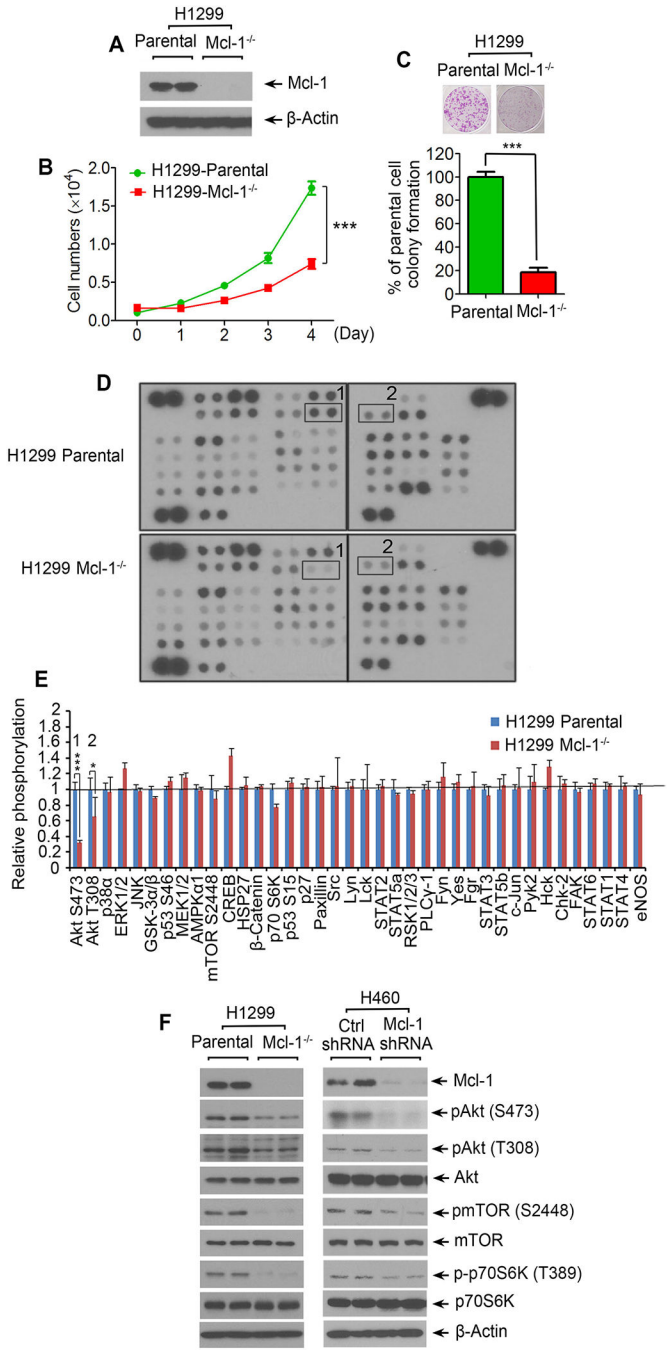

Figure 1.

Knockout of Mcl-1 suppresses cancer cell growth via downregulation of Akt activity. **A-E**, Mcl-1 was knocked out from H1299 cells using CRISPR/Cas9, followed by analysis of Mcl-1 expression by Western blot (**A**), growth curve (**B**), colony formation (**C**), human phospho-kinase array (1: Akt S473; 2: Akt T308) (**D**), and quantification of human phospho-kinase by image J (**E**). Data represent the mean ± SD. *$P < 0.05$, ***$P < 0.001$, by 2-tailed t test. (F) Mcl-1 was knocked out from H1299 cells, or knocked down from H460 cells, followed by Western blotting analysis of Mcl-1, pAkt, pmTOR and p-p70S6K.

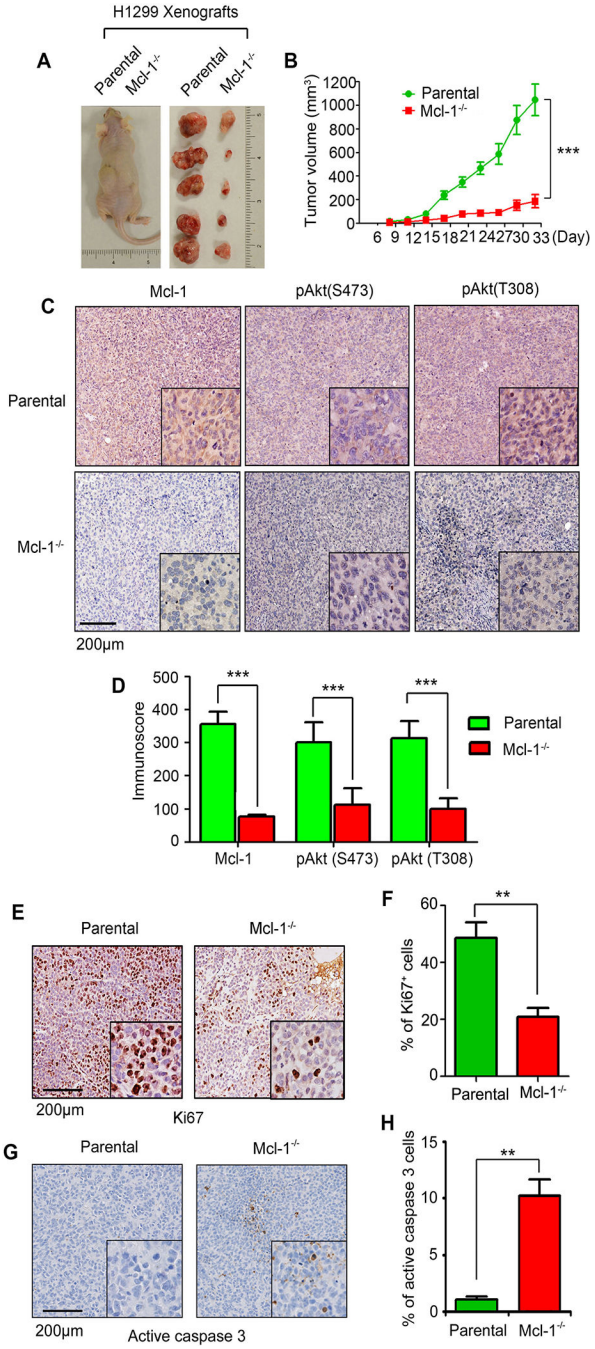

Figure 2.

Knockout of Mcl-1 inhibits tumor growth *in vivo*. **A** and **B**, The same number (3×10^6) of H1299 parental or Mcl-$1^{-/-}$ cells were injected into subcutaneous tissue in the flank region of nude mice to generate lung cancer xenografts (n=5 mice each group). Tumor volume was measured once every 3 days. After 33 days, the mice were sacrificed and the tumors were removed, photographed, and analyzed. Data represent the mean ± SD, n=5 per group. ***$P < 0.001$, by 2-tailed *t* test. **C-H**, IHC staining of Mcl-1, pAkt (S473), pAkt (T308), Ki67 and

active caspase 3 was performed in tumor tissues at the end of experiments. Data represent the mean ± SD, n=5 per group. $^{**}P < 0.01$, $^{***}P < 0.001$, by 2-tailed *t* test.

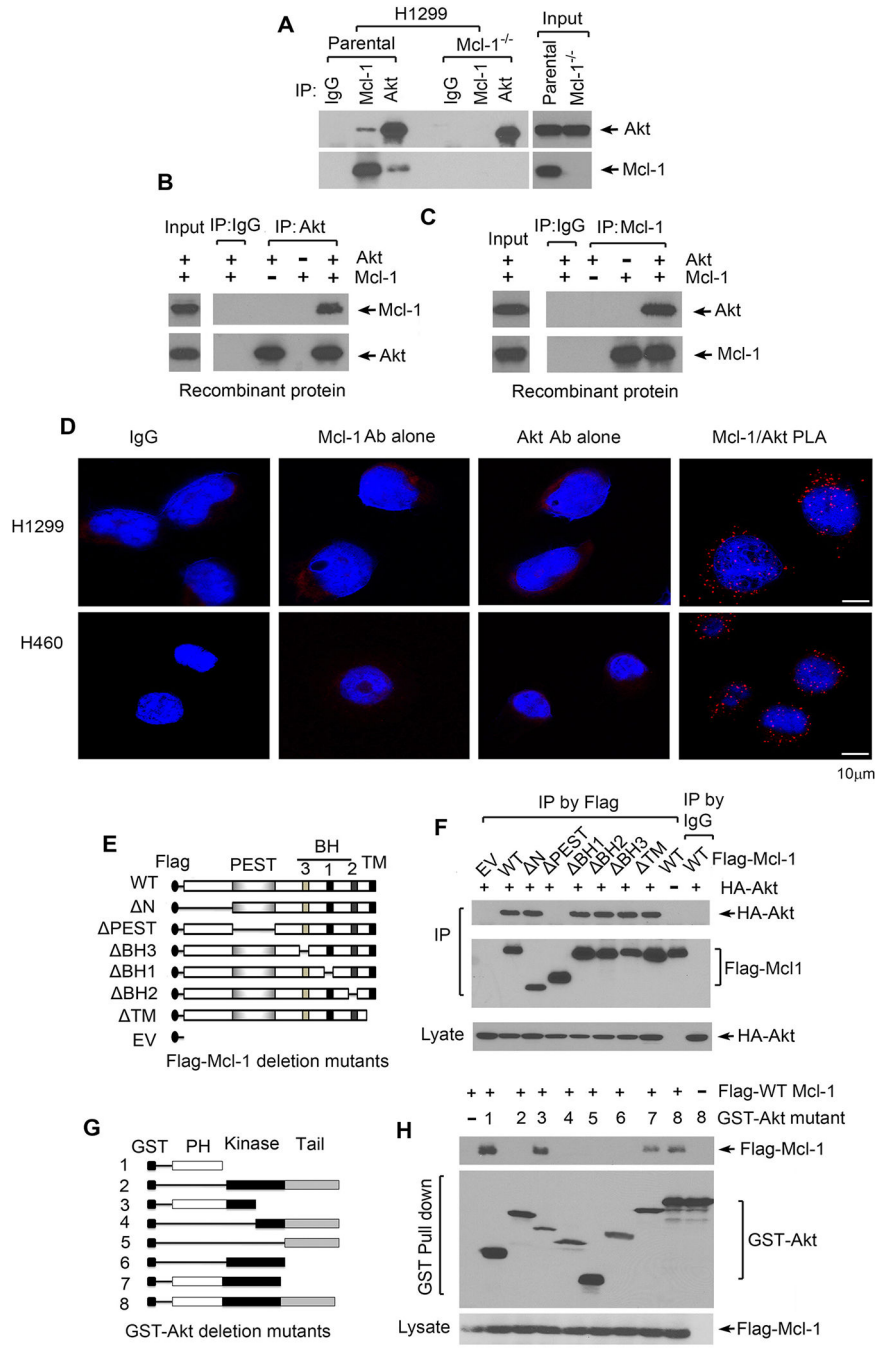

Figure 3.

Mcl-1 interacts via its PEST domain with Akt at its PH domain. **A**, Co-IP experiments were performed in H1299 vs. H1299 Mcl-1$^{-/-}$ cells using Mcl-1 or Akt antibody, followed by Western blot to measure endogenous Mcl-1/Akt interaction. IP by IgG was used as control. **B** and **C**, Co-IP experiments using Akt antibody or Mcl-1 antibody were performed in cell-free systems (recombinant His-tagged Akt and His-tagged Mcl-1 proteins in lysis buffer). **D**, Akt/Mcl-1 interactions were analyzed by the proximity ligation assay (PLA) in H1299 cells and H460 cells. PLA signals were detected by fluorescence microscopy as discrete spots.

IgG, single Akt antibody alone or single Mcl-1 antibody alone were used as negative control. **E**, Schematic representation of various Flag-tagged Mcl-1 deletion mutants. **F**, H1299 cells were co-transfected with HA-tagged WT Akt and various Flag-tagged Mcl-1 deletion mutants, followed by co-IP using Flag antibody and Western blot using HA or Flag antibody, respectively. **G**, Schematic representation of various GST-tagged Akt deletion mutants. **H**, H1299 cells were co-transfected with Flag-tagged WT Mcl-1 and various GST-tagged Akt deletion mutants, followed by GST pull down and Western blot using Flag or GST antibody, respectively.

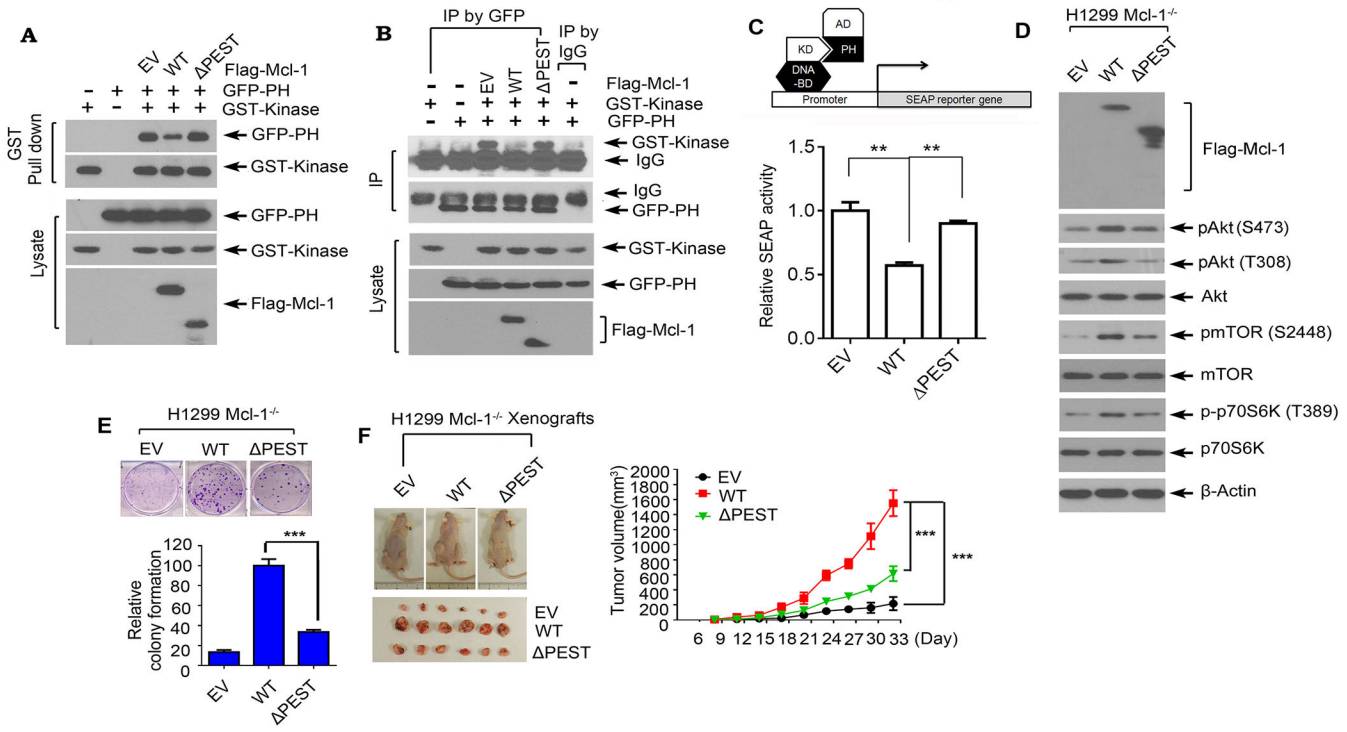

Figure 4.

The binding of Mcl-1 with Akt is essential for Mcl-1 to disrupt PH/KD interactions, upregulate Akt activity and promote tumor growth. **A** and **B**, GST-tagged kinase domain of Akt and GFP-tagged PH domain of Akt were co-transfected with Flag-tagged WT Mcl-1 or ΔPEST Mcl-1 mutant into H1299 cells, followed by GST pull down (**A**), or co-IP using GFP antibody (**B**), and Western blot using GST or GFP antibody. **C**, Interaction between the kinase domain and PH domain in the absence or presence of WT Mcl-1 or ΔPEST was measured in a mammalian two-hybrid system. **D** and **E**, H1299 Mcl-1$^{-/-}$ cells were transfected with empty vector (EV), Flag-tagged WT Mcl-1 or ΔPEST Mcl-1 mutant, followed by analysis of pAkt, pmTOR and p-p70 S6K by Western blot (**D**) and colony formation assay (**E**). Data represent the mean ± SD. ***$P < 0.001$, by 2-tailed t test. **F**, The same number (3×10^6) of H1299 Mcl-1$^{-/-}$ cells expressing EV, Flag-tagged WT Mcl-1 or ΔPEST mutant were injected into subcutaneous tissue in the flank region of nude mice to generate lung cancer xenografts. Tumor volume was measured once every 3 days. After 33 days, the mice were sacrificed and the tumors were removed, photographed, and analyzed. Data represent the mean ± SD, n=6 mice per group. ***$P < 0.001$, by 2-tailed t test.

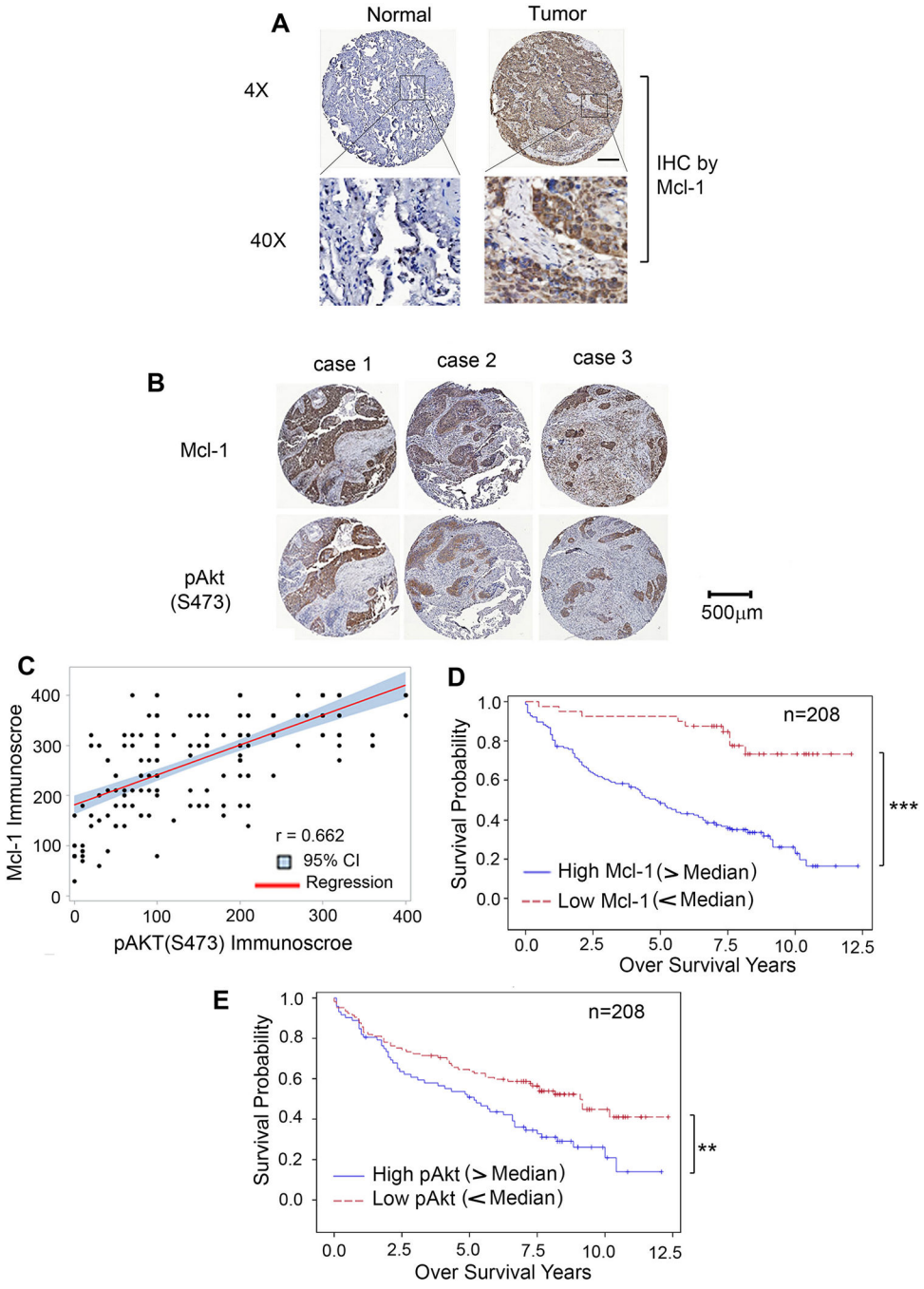

Figure 5.

Mcl-1 and pAkt are potential prognostic biomarkers for patients with NSCLC. **A**, Mcl-1 expression in normal lung tissues versus lung cancer tissues from a representative NSCLC case was analyzed by IHC using Mcl-1 antibody. Normal tissue is the adjacent normal lung tissue from the same case. Mcl-1 expression was quantified by immunoscore. **B**, IHC staining of Mcl-1 and pAkt (S473) was compared in tumor tissues from 3 representative NSCLC cases. **C**, The correlation between Mcl-1 and pAkt immunoscores in NSCLC patient tumors (n = 208) was explored using Pearson correlation analysis. Scatter plots of

Mcl-1 immunoscore and pAkt immunoscore were produced showing the fitted linear regression lines and 95% confidence intervals. **D** and **E**, Kaplan-Meier survival curves of NSCLC patients: low Mcl-1 vs. high Mcl-1 (**D**), low pAkt vs. high pAkt (**E**), n = 208. ***$P < 0.001$, **$P < 0.01$, by log-rank test. Low: immunoscore < 200, high: immunoscore > 200.

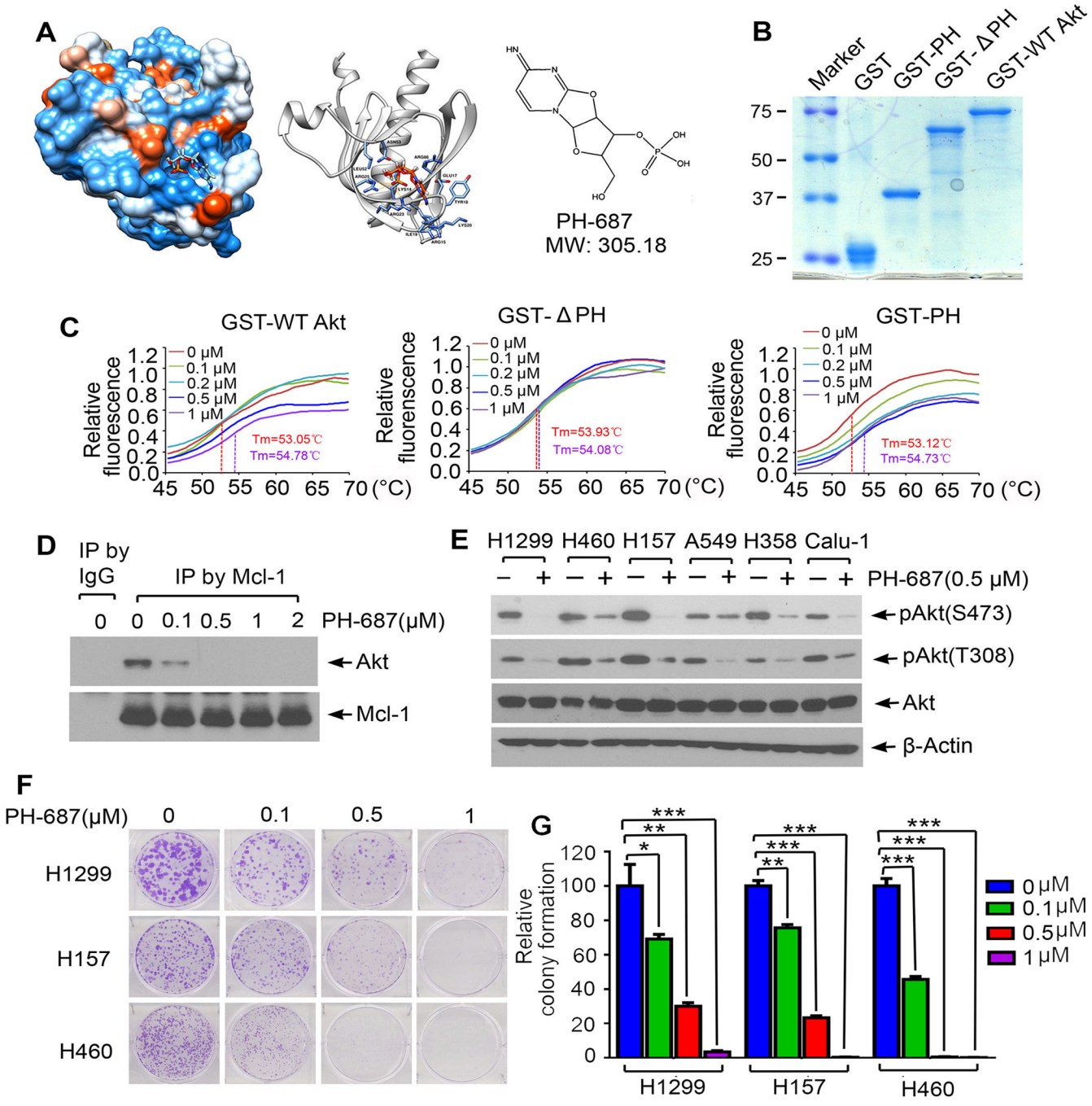

Figure 6.

Discovery of small molecule PH-687 as a lead compound that specifically binds to the PH domain of Akt, disrupts Mcl-1/Akt interaction and reduces Akt activity. **A**, Structural modeling of small molecule PH-687 in the PH domain binding pocket of Akt protein. **B**, Recombinant GST-PH, GST-ΔPH and GST-WT Akt recombinant proteins were purified from *Escherichia coli* Rosetta using glutathione sepharose column. Proteins were stained by Coomassie blue. **C**, Thermal shift melting curve of purified GST-WT Akt, GST-ΔPH and GST-PH-only proteins incubated with increasing concentrations of PH-687. Melting

temperature (Tm) values of 0μM and 1μM of PH-687 are shown. **D**, H1299 cells were treated with increasing concentrations of PH-687 for 24h, followed by co-IP using Mcl-1 antibody and Western blot with Akt or Mcl-1 antibody, respectively. **E**, Various lung cancer cell lines were treated with PH-687 (0.5 μM) for 24h, followed by analysis of pAkt by Western blot. **F** and **G**, Colony formation assay of H1299, H157 and H460 cells following treatment with increasing concentrations of PH-687. Data represent the mean ± SD. *$P <$ 0.05, **$P < 0.01$, ***$P < 0.001$, by 2-tailed t test.

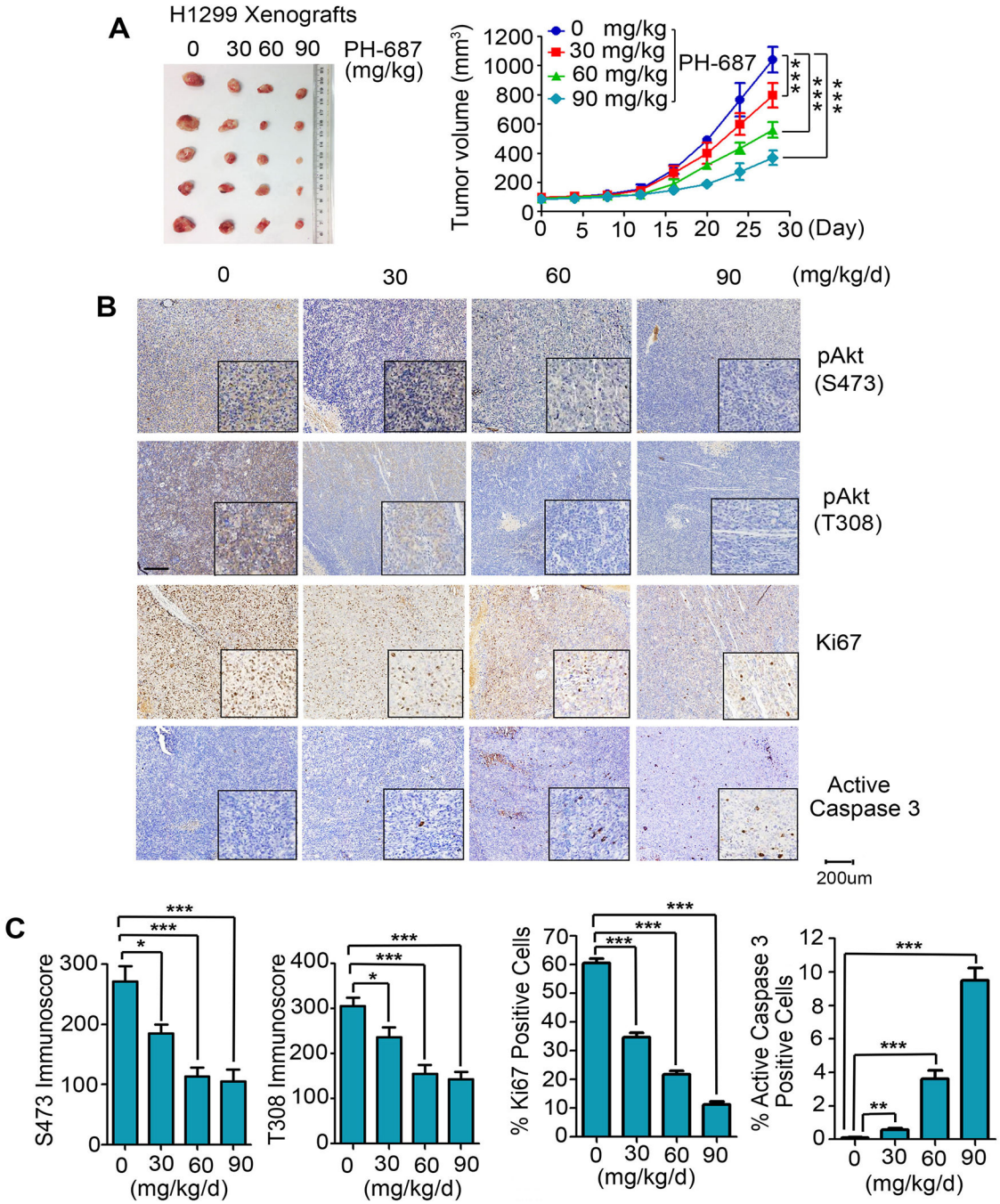

Figure 7.

PH-687 potently suppresses tumor growth *in vivo*. **A**, Nu/Nu nude mice with H1299 lung cancer xenografts were treated with increasing doses of PH-687 for 4 weeks. Tumor volume was measured once every 4 days. After 28 days, mice were sacrificed and the tumors were removed, photographed, and analyzed. Data represent the mean ± SD, n=5 per group. ***$P < 0.001$, by 2-tailed *t*-test. **B** and **C**, pAkt (S473), pAkt (T308), Ki67 and active caspase 3 in tumor tissues were analyzed by IHC staining at the end of experiments and quantified. Scale

bar represents 200 μm. Data represent the mean ± SD, n=5 per group. *$P < 0.05$, **$P < 0.01$ and ***$P < 0.001$, by 2-tailed *t*-test.